Linking dominant rainfall-runoff event hydrologic response dynamics with nitrate and chloride load estimates of three boreal Shield catchments

C. A. Ross[1], N. J. Casson[2], and M. Tenuwara[2]

[1]Department of Geography and Environmental Studies, Ryerson University, Toronto, Ontario, Canada.

[2]Department of Geography, University of Winnipeg, Winnipeg, Manitoba, Canada

Corresponding author: Nora Casson (n.casson@uwinnipeg.ca)

Main point #1:
Rainfall-runoff event analysis at boreal Shield catchments indicated significant temporal variability in hydrologic response & solute export

Main point #2:
Leveraging newly available tools for quasi-automated rainfall-runoff event delineation allows new insights to be gleaned from long-term data

Main point #3:
Classes of rainfall-runoff events characterized by response magnitude & timing are associated with significant differences in solute export

Plain Language Summary

The boreal region is a vast mosaic of freshwater resources, including wetlands, streams and lakes. The movement of water and solutes through catchments in this region is very sensitive to climate change, making it critical to understand the controls on these processes. Rainfall events are very important for transporting water and solutes from catchments to streams, and are particularly sensitive to changes in climate. It is difficult to understand event-scale dynamics since long records and high-frequency datasets are not common, and take a long time to process. The goal of this study was to look at event-scale chloride and nitrate dynamics from a long-term study site using recently-developed tools for delineating events. There was a lot of variability in streamflow responses to events, and summer and fall events were somewhat similar. There was a wide range of nitrate and chloride export associated with events, and some of the variability had to do not just with the magnitude of the event, but also with the timing. This study highlights the value of collecting high-frequency datasets at long-term study sites in order to understand the impacts of climate change in the boreal region.

This article has been accepted for publication and undergone full peer review but has not been through the copyediting, typesetting, pagination and proofreading process, which may lead to differences between this version and the Version of Record. Please cite this article as doi: 10.1029/2020JG006187.

Abstract

Understanding hydrological dynamics in boreal Shield catchments is critical for projecting changes in stream runoff and chemistry in a region that is sensitive to climate change. Previous work has mostly focused on a limited number of events over one or a few seasons because of the relative scarcity of high-frequency datasets and automated tools for rainfall-runoff event delineation. For the boreal region, a greater understanding of seasonality in hydrologic response and solute export related to rainfall-initiated events is needed, as significant shifts in hydrologic regime from climate change are expected. This study aimed to help resolve these knowledge gaps by assessing event-scale hydrologic response dynamics and stream loads of nitrate and chloride using long-term data from three boreal Shield catchments. Hydrometric and stream chemistry data from 2001-2018 were analyzed to delineate rainfall-runoff events and estimate event nitrate and chloride loads. Event hydrologic response and loads were highly variable, especially with respect to catchment runoff initiation. Only subtle differences in hydrologic response dynamics were observed between summer and fall events, while seasonal differences in event nitrate and chloride loads were mostly statistically significant. Interestingly, a wide range of rainfall-runoff events classified by response magnitude and timing were associated with differences in nitrate and chloride export. This study further confirms the utility of long-term high-frequency datasets and illustrates the need for additional work to further assess long-term changes in event-based hydrologic response and stream solute concentrations in the boreal region.

1 Introduction

Understanding relationships between hydrologic event response dynamics and solute export is of critical importance, as more solutes are typically transported from streams during transitory high-flow events compared to baseflow (Horowitz, 2013; Inamdar et al., 2006; Inamdar & Mitchell, 2006; Long et al., 2015; Macrae et al., 2007; Raymond & Saiers, 2010; Swistock et al., 1997). Relationships between hydrologic response and solute concentrations during hydrologic events are dynamic, nonlinear, and highly variable (Pellerin et al., 2012) and stream loads are strongly dependent on storm characteristics and antecedent conditions (Inamdar et al., 2004, 2006; Oswald & Branfireun, 2014). Insights into biogeochemical processes, including diagnostics and predicting solute mobilization and export, can be reached by evaluating catchment hydrologic response to meteorological inputs across multiple rainfall-runoff events (Creed & Band, 1998; Inamdar & Mitchell, 2006).

Analyses of catchment hydrologic response to individual rainfall events have informed hypotheses of catchment function and provide insights on runoff generation processes and their temporal dynamics (Blume et al., 2007; McDonnell et al., 2007; Tarasova et al., 2018). The variability of runoff response to rainfall events influences both downstream water and solute delivery (James & Roulet, 2007; Stieglitz et al., 2003; Tarasova et al., 2018). A wide range of response metrics can be derived during rainfall-runoff analyses that show the influence of physiographic and climatic controls on hydrologic responses (Te Chow, 1959) and provide first-order information on hydrologic function (Carey & Woo, 2001; Ross et al., 2019; Tang & Carey,

2017). These metrics quantify the magnitude and timing of response and may contribute to enhancing biogeochemical process understanding.

Previous work evaluating biogeochemical processes at the rainfall-runoff event scale has shown that the expression of some solutes may vary seasonally, especially with changes in antecedent conditions, and characteristics of rainfall-runoff events (Inamdar et al., 2004). Stream solute dynamics at catchment outlets are a function of interactions between transport via hydrological flowpaths and the characteristics of source areas of solutes across the catchment (Basu et al., 2010). Both source and transport dynamics vary in space and time, which gives rise to complex relationships. Source characteristics that influence this relationship include the spatial arrangement of locations throughout the catchment (McGlynn & McDonnell, 2003); the biogeochemical environment of the source location (e.g. redox conditions which lead to consumption or production of the solute) (McClain et al., 2003); how biologically reactive the solute is (Duncan et al., 2017); and the ratio of supply to demand of the particular solute (Creed et al., 1996). While these source areas can occur heterogeneously throughout the catchment, the riparian or near-stream zone is often a critical control point for determining stream solute patterns (Allan et al., 1993; Casson et al., 2019; Cirmo & McDonnell, 1997). Contrasting biologically reactive or redox-sensitive solutes (e.g. nitrate; NO_3-N) with less reactive solutes (e.g. chloride; Cl) can help to tease apart the relative influence of hydrologic vs. biogeochemical controls on patterns of stream solute chemistry (Moatar et al., 2017).

Motivation to better understand relationships between event hydrologic response and solute export is intensified by observed shifts in hydrologic regime related to climate change (Whitfield & Cannon, 2000). In the boreal region, these changes are especially impactful, as the seasonal streamflow regime exhibits considerable inter-annual variability and is susceptible to climate-related stressors (Woo et al., 2008). By characterizing and comparing rainfall-runoff response for multiple catchments, we can evaluate catchment resilience to stressors that influence streamflow and related processes (Carey et al., 2010). Such comparisons can also contribute insights into the relative importance of dynamic, climate-related controls, and fixed physiographic controls on catchment response (Devito et al., 2005). While there are benefits to understanding relationships between hydrologic response dynamics and solute export at the event scale, such analyses require high-frequency data and considerable effort. The scarcity of long-term high-frequency datasets and automated tools for event delineation have impeded efforts to explore these relationships. This paper aims to help resolve this knowledge gap by assessing event-scale hydrologic dynamics and event solute loads using long-term data from three boreal Shield catchments. The focus is on three research questions:

1. Does event hydrological response vary by catchment and/or season?
2. Do event nitrate and chloride loads vary by catchment and/or seasons?
3. Do events that are characterized by different hydrologic response magnitudes and timing also differ in terms of solute export?

2 Methods

2.1 Site description

This study focuses on three small forested catchments that drain into Lake 239 (Figure 1) of the International Institute for Sustainable Development Experimental Lakes Area (IISD-ELA), which is located approximately 55 km southeast of Kenora, Ontario, Canada (Brunskill & Schindler, 1971; Parker et al., 2009; Schindler et al., 1996). These catchments are part of long-term streamflow and chemistry monitoring efforts. Soils of the area are primarily thin (<1 m in depth) orthic brunisols that cover pink Precambrian granodiorite (Brunskill & Schindler, 1971; Parker et al., 2009). These catchments have not been logged or managed, but forests have been affected at varying degrees by windstorms and fire (Emmerton et al., 2019). In general, forest cover becomes denser towards the lower portions of the catchments and primarily consists of old-grown *Pinus banksiana*, *Picea glauca*, and *Picea mariana* (Brunskill & Schindler, 1971; Parker et al., 2009).

The three study catchments vary in size and wetland extent. The northeast catchment (NEIF) is the smallest (12 ha), but has the greatest proportion of wetland (30%): a wooded Sphagnum bog at the base of the catchment, surrounding the stream (Brunskill & Schindler, 1971; Parker et al., 2009; Schindler et al., 1996). The northwest catchment (NWIF) is medium in size (56 ha), with a gently-sloping upland and a small wetland (3.5%) near the catchment outlet. The east catchment (EIF) is the largest (170 ha), with a small wetland (4%) located in the upper portion of the catchment. The lower section of the EIF has a deeper (up to 10 m) glacial overburden with quaternary deposits of sand and till (Schindler et al., 1996).

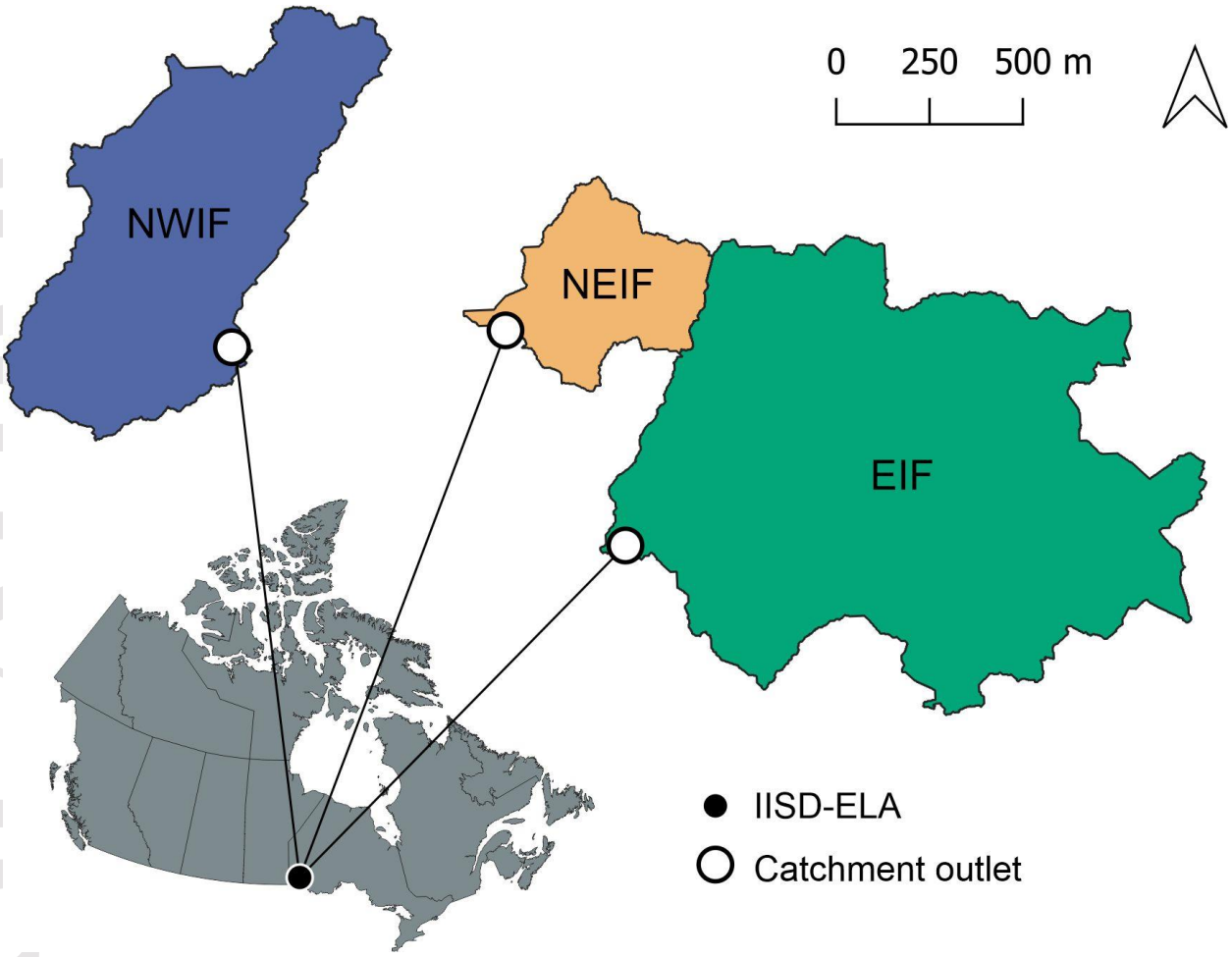

Figure 1. Location of the IISD-ELA within Canada and the configuration of the NWIF, NEIF, and EIF catchments of Lake 239.

2.2 Rainfall-runoff event delineation

For the EIF, NEIF, and NWIF catchments, high-frequency (HF) discharge data (10-minute) and rainfall data (1-hour) from 2001 to 2018 (except for interrupted sampling in 2008) were analyzed to identify rainfall-runoff events. While the data record at ELA starts in the 1970s, the HF record is only available starting in 2001. This period corresponds with a more intense wet period at the ELA site compared with the long-term average, resulting from a positive phase in decadal climate signals as well as an increase in regional total precipitation (Emmerton et al., 2019). For synchronicity between discharge and rainfall, discharge data were aggregated to a 1-hour time-step by the mean. Rainfall and runoff events were identified and matched using the MATLAB toolbox HydRun (Tang & Carey, 2017). Sequential rainfall observations separated by a rainless period shorter than 24 hours were considered rainfall events, and runoff events were identified based on the hydrograph shape (Tang & Carey, 2017). Some events were discarded since they had runoff ratios greater than one and/or hydrograph response before rainfall, which we ascribed to delineation errors. In total, 372 rainfall-runoff events were retained: 106, 129, and 137 for the EIF, NEIF, and NWIF, respectively. While snowmelt is hydrologically relevant in the

region, this research was limited to rainfall-runoff events: hydrologic responses initiated by snowmelt or rain-on-snow were not considered. Rainfall-runoff events were coarsely grouped into seasonal categories based on the event start date: events that started between May and August were considered summer events, and events that started between September and November were considered fall events.

2.3 Characterization of event hydrologic response

Each event was characterized using two types of hydrologic response metrics: response magnitude metrics (magnitude metrics) and response timing metrics (timing metrics). Magnitude metrics include the total event runoff (Q_{TOT}), peak discharge (Q_{MAX}), runoff ratio (RR), and initial abstraction (I_{abs}). Q_{TOT} was normalized by the catchment drainage area. The RR represents the fraction of event rainfall that becomes runoff and I_{abs} estimates storage as the amount of rain falling before the initial hydrograph rise (Dingman, 2015). Timing metrics include the time of hydrograph rise (T_r), response lag (T_{LR}), lag-to-peak (T_{LP}), centroid lag (T_{LC}), and time of concentration (T_c). Timing metrics capture durations of time between distinct features of the event hyetograph and hydrograph: T_r is the time from the start of the hydrograph rise to the peak discharge; T_{LR} and T_{LP} are the durations between the beginning of rainfall and the initial hydrograph rise and peak discharge, respectively; T_{LC} is the time elapsed between centroids of the hydrograph and hyetograph; and T_c is the amount of time from the end of rainfall to the end of the event response (Dingman, 2015). Site- and season-specific response metric summary statistics were computed, including measures of central tendency (i.e., mean, median) and dispersion (i.e., minimum, maximum, standard deviation, and coefficient of variation). These summary statistics were compared to assess whether event responses varied by site and/or season (research question 1). Differences in response metric distributions between sites and between seasons at individual sites were further assessed using the Kruskal-Wallis H tests (Vargha & Delaney, 1998).

Events were classified using key response metrics in an empirical classification space to identify the dominant type of rainfall-runoff event for each site (Ross et al., 2019). Principal component analysis (PCA) was performed for each site to identify the response metrics that best illustrate response variability. PCA transforms data into uncorrelated principal components (PCs), which are ordered by the amount of variance captured compared to the original data (Legendre & Legendre, 2012). The first three PCs were retained to ensure that a high percentage of the response variability was captured. For each site, the PC loadings were evaluated to assess the contribution of each original response metric to the variance explained by each PC (Legendre & Legendre, 2012; Ross et al., 2019). The response magnitude metric and the response timing metric with the maximum loading across the first three PCs for all sites were identified as the metrics that best capture response variability. These metrics were used to classify rainfall-runoff event responses using scatter plots showing response magnitude (x-axis) and response timing (y-axis). Notably, such classification spaces do not suggest causal relationships between magnitude and timing metrics. The x-axis and y-axis were segmented by the median of their respective response metric, leading to a four-quadrant classification space (Ross et al., 2019). For each site, events that plot in the lower left quadrant (Q1) are low-magnitude and fast-timing, events that plot in the lower right quadrant (Q2) are high-magnitude and fast-timing, events that plot in the upper right quadrant (Q3) are high-magnitude and slow-timing, and events that plot in the upper left quadrant (Q4) are low-magnitude and slow-timing.

2.4 Event nitrate and chloride load estimates

The available chemistry data were from grab samples taken at each site approximately every two weeks during the summer and fall. The NO_3-N and Cl concentrations (mg/L) of grab samples were assumed to be representative of the average solute concentrations of the day that they were collected. Site-specific chemistry and discharge data were separated by season. The HF discharge timeseries for each site and season were aggregated to a daily mean discharge timeseries and their associated flow duration curves were computed. Chemistry data were then matched to their associated flow duration curves by date to assess the range of flow conditions with chemistry data (Figure S1). The paired chemistry and daily mean discharge data were used to develop and calibrate site- and season-specific regression models for estimating daily NO_3-N and Cl loads (g/day) using LOADEST, as implemented in the rloadest package for R . These models included the centred, log-transformed discharge and the centred decimal time as predictor variables. The discharge was log-transformed and centred to normalize the data, to account for the influence of outliers, and to mitigate the influence of multicollinearity (Runkel et al., 2004). The decimal time was included to account for potential trend present in the long-term record. Predictor variables to account for seasonality were not included, since summer and fall models were calibrated independently. Results from model calibration were assessed using standard regression diagnostics (e.g., quantile-quantile plots, parameter significance, variance inflation factors). The associated fit of these models, as indicated by the R^2, ranged from 0.57 to 0.95. In general, the R^2 of models for Cl (R^2: 0.82 – 0.95) were greater than that of models for NO_3-N (R^2: 0.57 – 0.75). Regardless of constituent, the R^2 values of fall models (R^2: 0.64 – 0.95) were greater than that of summer models (R^2: 0.57 – 0.88). Additionally, the sparser two-week chemistry data interval prevented issues of autocorrelation related to samples that are taken within seven days of one another (Runkel et al., 2004). These site- and season-specific models were used to predict daily NO_3-N and Cl loads (g/day) for the study period, which were then normalized by the catchment area (g/ha/day).

For each rainfall-runoff event, event days were determined based on the start and end time of event hydrologic response that was determined during event delineation. The event days were used to match the event with the associated daily NO_3-N and Cl load estimates. These daily load estimates were summed to obtain an event load estimate. For events associated with partial days, the proportion of the day associated with event hydrologic response was used directly to calculate the proportion of the daily solute load to be considered in the event load estimate. For example, an event with response starting 2001-05-01 12:00:00 and ending 2001-05-03 16:00:00 with daily loads of 2 g/ha on 2001-05-01, 2g/ha on 2001-05-02, and 2g/ha 2001-05-3, would have an event load estimate equal to (2g/ha x (24hrs – 12hrs)/24hrs) + (2 g/ha x 24hrs/24hrs) + (2g/ha x 16hrs/24hrs). Like event hydrologic responses, NO_3-N and Cl load estimates of different sites and seasons were compared using summary statistics and the Kruskal-Wallis H test (research question 2). Importantly, event load estimates were also assessed with respect to event hydrologic response classification using the Kruskal-Wallis H test and pairwise Wilcoxon rank sum tests to ascertain whether load estimates differed by event class (research question 3).

3 Results

3.1 Event hydrologic response dynamics

Summary statistics of event magnitude and timing metrics for the EIF, NEIF, and NWIF are shown in Table 1. There was considerable inter-event variability in magnitude metrics, as indicated by high levels of dispersion around metric means (CV: 0.77 – 2.10). Event I_{abs} were similar across sites. The largest median and maximum event Q_{TOT} were observed at the NEIF, however, differences in the distributions of event Q_{TOT} between sites were not statistically significant. In contrast, metric-specific Kruskal-Wallis tests showed that differences in the distributions of Q_{MAX} (H = 141.89; p-value = 0.00) and RR (H = 7.57; p-value = 0.02) between sites were statistically significant. For these tests, the null hypothesis is that the distribution of the response metric are the same for each site, while the alternative hypothesis is that the distribution differs for at least one site (Hollander et al., 2013). There were no statistically significant differences between the event response timing metric distributions of sites.

Table 1. Summary statistics of event response magnitude and response timing metrics for EIF, NEIF, and NWIF catchments. SD: standard deviation, CV: coefficient of variation.

		Response magnitude metrics				Response timing metrics				
		Q_{TOT} (mm)	Q_{MAX} (m^3/s)	RR (-)	I_{abs} (mm)	T_r (hrs)	T_{LR} (hrs)	T_{LP} (hrs)	T_{LC} (hrs)	T_c (hrs)
EIF	Mean	6.07	0.10	0.15	14.03	22.76	59.98	82.74	45.87	56.58
	Median	3.29	0.03	0.11	6.35	21.00	57.00	80.50	38.10	55.00
	Minimum	0.23	0.00	0.00	0.00	3.00	0.00	4.00	7.34	2.00
	Maximum	54.70	1.45	0.69	77.80	79.00	256.00	281.00	163.12	154.00
	SD	8.49	0.21	0.15	19.13	16.45	48.55	52.17	27.21	30.40
	CV	1.40	2.10	1.00	1.36	0.72	0.81	0.63	0.59	0.54
NEIF	Mean	6.91	0.01	0.18	13.77	21.78	62.83	84.59	49.25	62.16
	Median	4.64	0.00	0.14	5.60	17.00	57.50	80.50	41.00	57.00
	Minimum	0.42	0.00	0.01	0.00	5.00	0.00	8.00	11.34	0.00
	Maximum	61.63	0.04	0.83	97.50	93.00	251.00	281.00	161.09	159.00
	SD	9.26	0.01	0.13	18.30	14.32	54.24	55.44	28.05	31.77
	CV	1.34	0.97	0.77	1.33	0.66	0.86	0.66	0.57	0.51
NWIF	Mean	6.42	0.03	0.16	12.77	26.49	56.19	82.62	45.85	64.13
	Median	2.98	0.01	0.11	4.70	19.00	55.00	76.00	36.16	54.00
	Minimum	0.17	0.00	0.01	0.00	5.00	0.00	7.00	0.95	4.00
	Maximum	45.03	0.42	0.66	77.80	159.00	256.00	288.00	156.26	216.00
	SD	8.57	0.06	0.16	18.33	20.99	48.96	53.16	28.02	37.69

	CV	1.34	1.80	0.98	1.44	0.79	0.87	0.64	0.61	0.59

Violin plots in Figure 2 show the distributions of select magnitude and timing metrics for summer and fall events. For all sites, the Q_{TOT} and Q_{MAX} of summer events generally covered a wider range than fall events. The range and maximum values of RR and I_{abs} were typically larger for summer events. Differences between the distributions of summer and fall event magnitude metrics were only statistically significant for RR (H = 4.30; p-value = 0.04) and I_{abs} (H = 4.55; p-value = 0.03) at the NEIF. Seasonal differences in timing metrics were realtively small (Figure 3). Differences in the distribution of response timing metrics by season were only statistically significant at the NEIF site, and only for T_c (H = 6.32, p-value = 0.01).

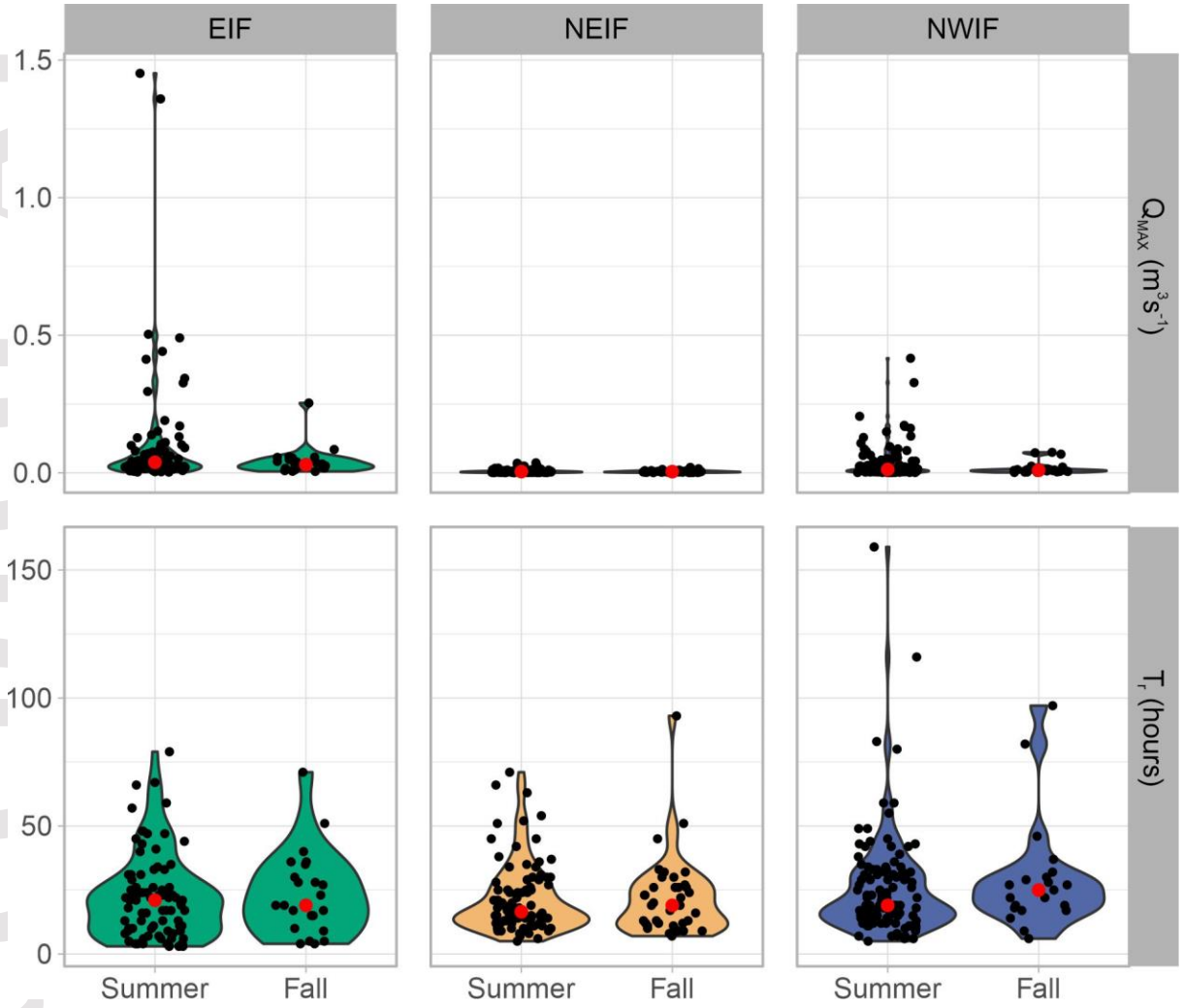

Figure 2. Violin plots showing the distribution of Q_{MAX} and T_r for summer and fall events at each site. Red dots show median metric values and black dots show individual events.

The site-specific PCA showed that between 77% and 79% of the response variance was explained by the first three principal components (PCs) (Table 2). Metric-specific loadings for

the first three PCs indicate which metrics are most important for explaining temporal variability in response at each site. Regardless of the site, Q_{MAX} had the largest loading mean across the first three PCs. Q_{TOT} also had a relatively large loading mean across the first three PCs, while that of RR was comparatively small. The relative importance of I_{abs} for explaining response variability differed across sites: I_{abs} had a large average PC loading across the first three PCs at the EIF (mean = 0.26) and NWIF (mean = 0.30), but not the NEIF (mean = 0.18). For timing metrics, each metric had PC loadings greater than |0.45| for at least one of the first three PCs at all sites. Only the T_r and T_{LR} metrics had large mean PC loadings across the first three PCs for all sites – overall, T_r had the largest individual loading and the largest mean loading across the first three PCs for all sites. For each site, event hydrologic responses were classified using an empirical classification space (Section 2.2) with Q_{MAX} on the x-axis and T_r on the y-axis (Figure 3). For all sites, event responses were dominantly low-magnitude and fast-timing (Q1). The separation of the empirical classification space by season showed differences in response classes for summer and fall events (Figure 3). Regardless of site, most events with high-magnitude response (i.e., Q2 and Q3) occurred during the summer. For the NEIF and NWIF, summer events appear less variable in terms of response classification than fall events.

Table 2. Site-specific results of principal component analysis. Eigenvalues, the proportion of variance explained by the first three PCs, and the cumulative proportion of variance explained are shown in the upper section of the table. The absolute value of metric-specific loadings for the first 3 principal components are shown in the lower portion of the table. P: proportion; PC: principal component.

	EIF			NEIF			NWIF		
	PC1	PC2	PC3	PC1	PC2	PC3	PC1	PC2	PC3
Eigenvalue	3.12	2.63	1.38	3.22	2.65	1.13	3.00	2.67	1.26
P explained	0.35	0.29	0.15	0.36	0.29	0.13	0.33	0.30	0.14
Cumulative P	0.35	0.64	0.79	0.36	0.65	0.78	0.33	0.63	0.77
					PC loadings				
Q_{TOT}	0.14	0.58	0.10	0.11	0.55	0.05	0.12	0.57	0.21
Q_{MAX}	0.11	0.54	0.24	0.11	0.54	0.19	0.10	0.51	0.42
RR	0.01	0.53	0.06	0.26	0.43	0.02	0.01	0.53	0.11
I_{abs}	0.38	0.04	0.35	0.41	0.12	0.02	0.41	0.11	0.37
T_r	0.18	0.23	0.59	0.05	0.15	0.86	0.15	0.23	0.54
T_{LR}	0.51	0.13	0.16	0.52	0.12	0.07	0.51	0.14	0.14
T_{LP}	0.53	0.05	0.04	0.49	0.15	0.29	0.53	0.04	0.09
T_{LC}	0.49	0.16	0.15	0.47	0.18	0.03	0.48	0.08	0.26
T_c	0.09	0.02	0.64	0.09	0.35	0.03	0.07	0.22	0.50

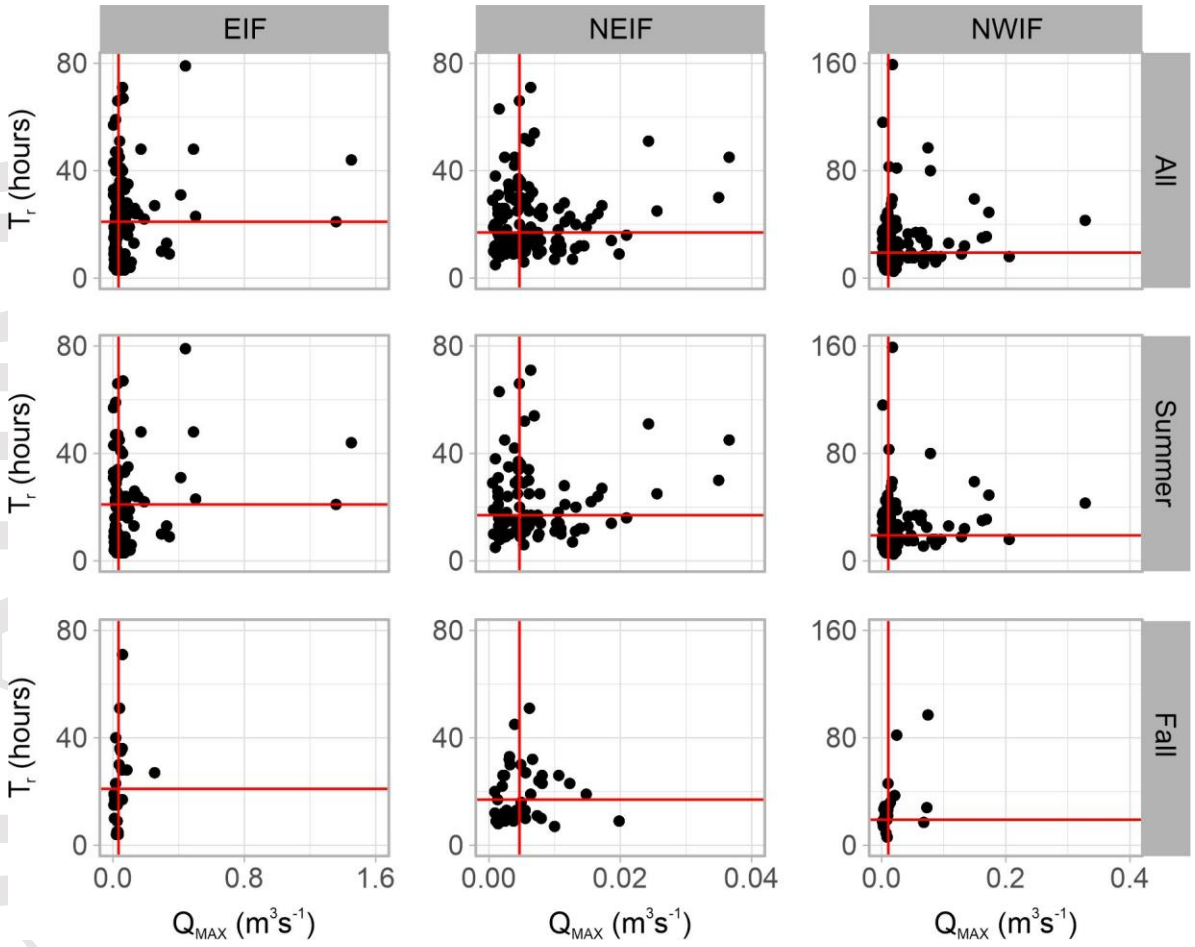

Figure 3. Site-specific empirical classification spaces constructed with Q_{MAX} and T_r. Dots are individual events and red lines show the median value of the associated metric. Events in the lower left quadrant (Q1) are low-magnitude and fast-timing, events in the lower right quadrant (Q2) are high-magnitude and fast-timing, events in the upper right quadrant (Q3) are high-magnitude and slow-timing, and events in the upper left quadrant (Q4) are low-magnitude and slow-timing.

3.2 Event nitrate and chloride load estimates

The area-normalized event NO_3-N and Cl load estimates and their associated summary statistics are shown in Figure 4 and Table 3, respectively. Kruskal-Wallis H tests showed statistically significant differences in the distributions of event NO_3-N (H = 246.79; p-value = 0.00) and Cl loads (H = 140.95; p-value = 0.00) between sites. The NO_3-N and Cl load estimates varied among events for each site, as indicated by the standard deviation and coefficient of variation. The mean, median, and maximum area-normalized NO_3-N loads were largest at the EIF, followed by the NWIF, and NEIF, consistent with literature demonstrating that the proportion and location of catchment wetland coverage are highly correlated with NO_3-N loads (Creed et al. 1998; Casson et al. 2019). In terms of the area-normalized Cl load estimates, the maximum area-normalized Cl load was largest for the NWIF followed by the EIF, and NEIF

sites. There were also minor differences in the mean and median area-normalized Cl load estimates of the three sites.

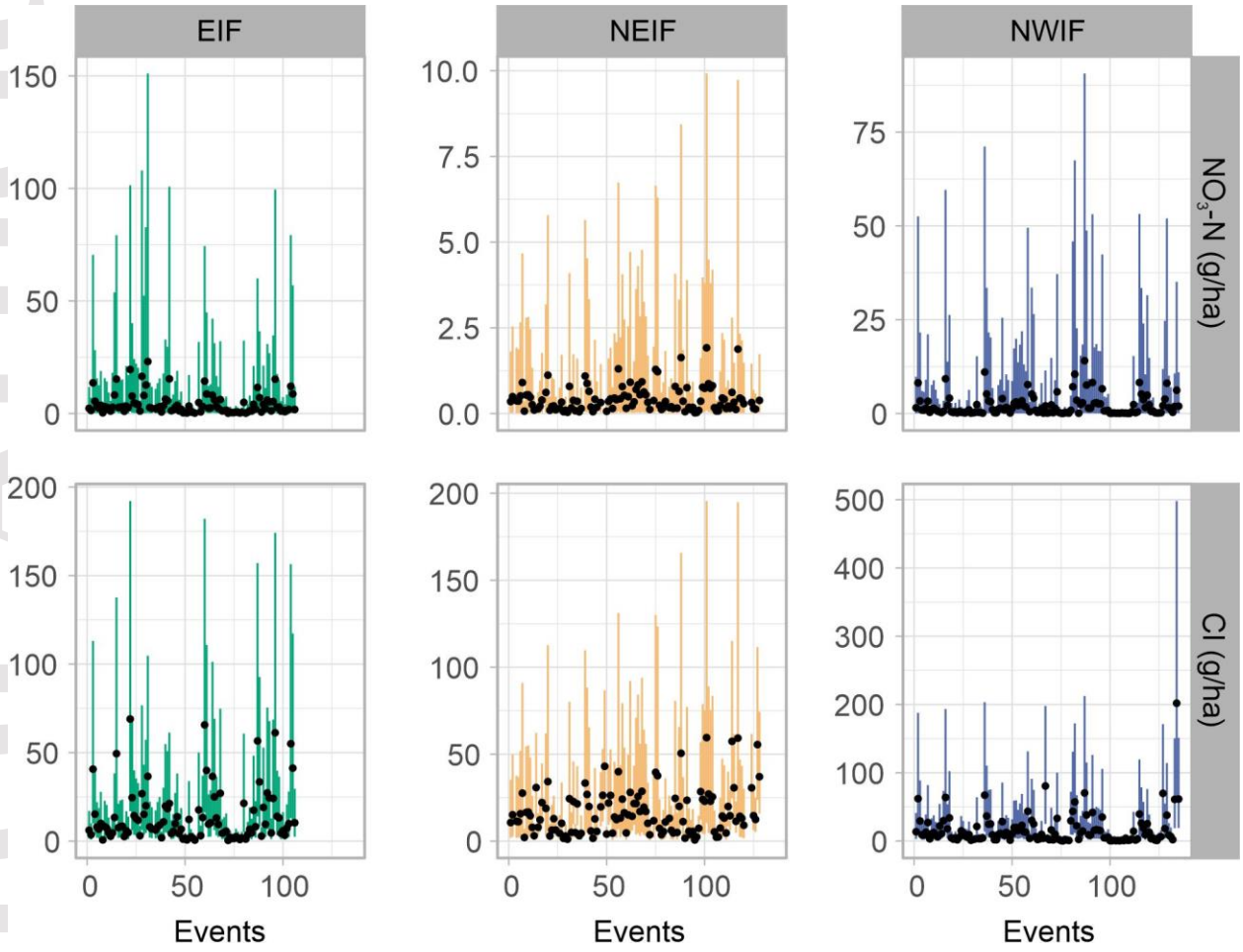

Figure 4. Site-specific area-normalized event NO_3-N and Cl export estimates with colour-coded prediction intervals (95%) for each event.

Table 3. Summary statistics of area-normalized NO_3-N and Cl load estimates for all events, summer events, and fall events of the EIF, NEIF, and NWIF. SD: standard deviation, CV: coefficient of variation.

		NO_3-N (g/ha)			Cl (g/ha)		
		All	Summer	Fall	All	Summer	Fall
EIF	Mean	4.07	3.30	6.97	13.67	12.8	19.23
	Median	2.63	2.33	4.91	8.22	7.81	14.62
	Minimum	0.14	0.14	0.16	0.50	0.50	1.20
	Maximum	23.08	19.55	23.08	69.00	69.00	61.23
	SD	4.56	3.64	6.32	14.96	14.30	16.36
	CV	1.12	1.10	0.91	1.09	1.17	0.85
NEIF	Mean	0.43	0.49	0.24	16.61	15.13	20.59
	Median	0.35	0.41	0.22	13.60	12.64	19.84
	Minimum	0.02	0.02	0.03	0.71	0.71	2.46
	Maximum	1.92	1.92	0.62	59.54	59.54	57.40
	SD	0.38	0.41	0.14	13.10	12.59	13.83
	CV	1.74	0.83	0.59	0.79	0.83	0.67
NWIF	Mean	2.04	2.26	0.86	16.88	14.42	30.24
	Median	0.99	1.30	0.22	9.48	9.39	10.78
	Minimum	0.04	0.04	0.04	0.36	0.36	1.20
	Maximum	14.07	14.07	6.19	201.84	70.40	201.84
	SD	2.62	2.74	1.42	23.67	15.53	46.57
	CV	1.29	1.21	1.66	1.40	1.08	1.54

Seasonal differences in area-normalized event NO_3-N and Cl load estimates varied across sites. For the EIF, NO_3-N loads were greater for fall events than summer events, while the opposite was true for the NEIF and NWIF. Differences in NO_3-N load distributions for summer and fall events were statistically significant for the EIF ($H = 7.28$; p-value = 0.01), NEIF ($H = 9.17$; p-value = 0.00), and NWIF ($H = 10.35$; p-value = 0.00). Differences in Cl load distributions for summer and fall events were statistically significant for the EIF ($H = 6.37$; p-value = 0.01) and NEIF ($H = 4.86$; p-value = 0.03), but not the NWIF ($H = 1.32$; p-value = 0.26). The average Cl load of fall events was greater than that of summer events for all sites, however, the maximum Cl export was observed during the summer for the EIF and NEIF.

3.3 Event hydrologic response classification and NO_3-N and Cl loads

Figure 5 shows the distributions of area-normalized NO_3-N and Cl loads for events with different hydrologic response classifications (see Section 3.1). The load distributions for events with low-magnitude response (i.e., Q1 or Q4) were similar, regardless of solute or site. In contrast, load estimates for high-magnitude events (i.e., Q2 or Q3) are larger and more variable. It also appears that the median load estimates are largest for events with high-magnitude and slow-timing (i.e., Q3). Kruskal-Wallis H tests showed that regardless of site and solute, differences between load estimates for events of different hydrologic response classes were statistically significant (H statistics: 45.78 - 82.24; p-values < 0.00). Additional analysis comprising pairwise Wilcoxon rank sum tests showed that differences between NO_3-N and Cl load estimates between events of different hydrologic response class pairs for each site were mostly statistically significant (i.e., p-values < 0.046). In fact, this was true for all cases, except for the NO_3-N load estimates of events classified as high-magnitude and fast-timing (Q2) or high-magnitude and slow-timing (Q3) at NEIF (p-value = 0.11).

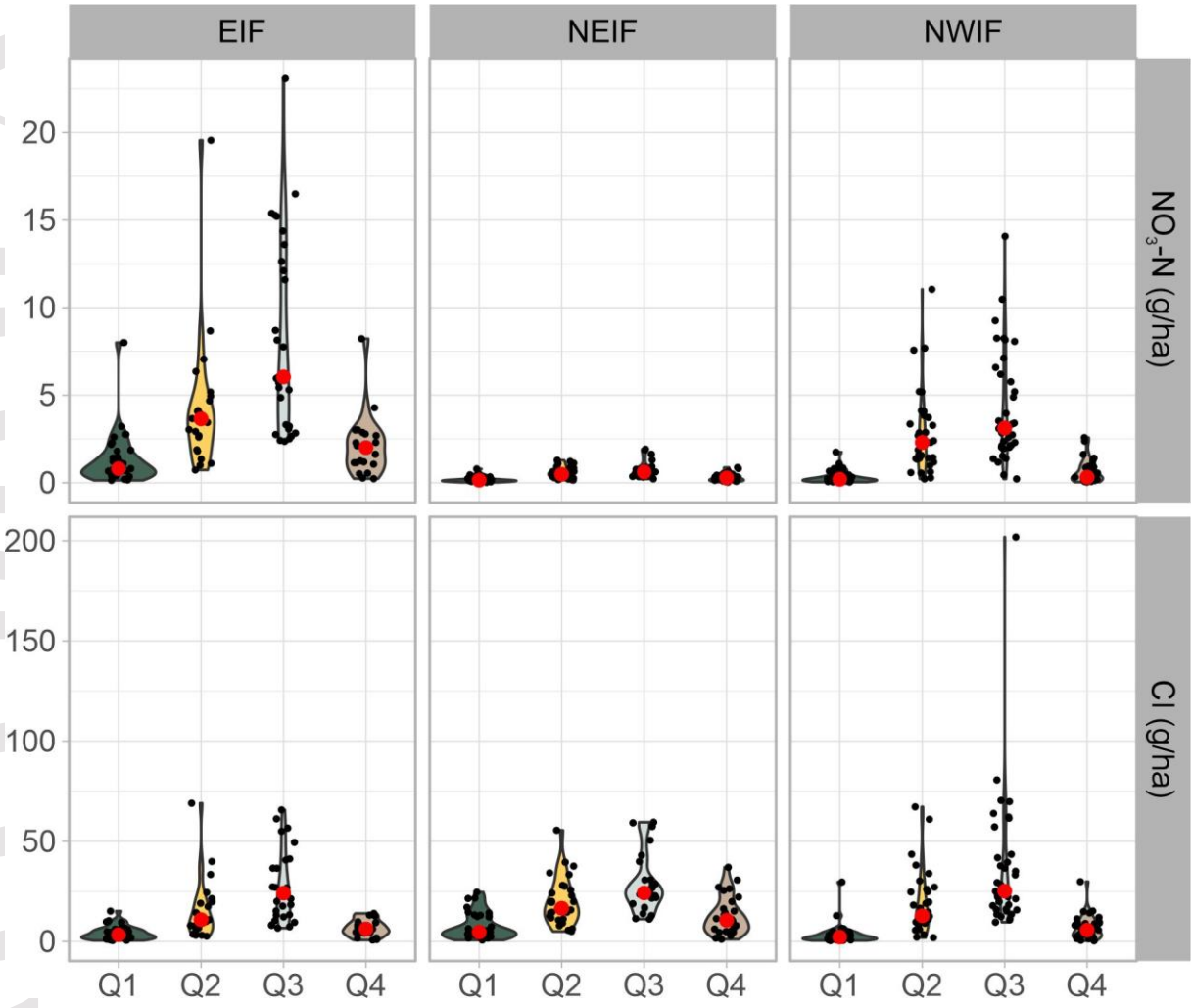

Figure 5. Violin plots showing the distributions of NO_3-N and Cl load estimates for events of each response classification. Response classifications are represented by quadrant: Q1 = low-

magnitude and fast-timing; Q2 = high-magnitude and fast-timing; Q3 = high-magnitude and slow-timing and Q4 = low-magnitude and slow-timing.

4 Discussion

This study aimed to leverage long-term hydrometric and stream chemistry data to better understand hydrologic response dynamics and solute loads of boreal Shield catchments. Indeed, other studies have successfully characterized rainfall-runoff event response dynamics (Allan & Roulet, 1994; Branfireun & Roulet, 1998; Frisbee et al., 2007; Oswald et al., 2011) and estimated nutrient loads (Casson et al., 2012; Eimers et al., 2011; Jager et al., 2009) for other boreal Shield catchments. With that said, investigations at the event scale typically assess relatively few events spanning one season to a few years at most. This is largely due to the scarcity of longer-term, high-frequency datasets and tools that facilitate automated rainfall-runoff event delineation (Ross et al., 2019). Furthermore, studies for boreal Shield catchments have often focused on snowmelt-initiated hydrologic responses. While snowmelt is important for boreal Shield catchments, their hydrologic regimes are expected to become more influenced by rainfall because of stressors from climate change (Emmerton et al., 2019). Therefore, this study is novel in two important ways. (1) The focus of this study was on hydrologic response dynamics and nitrate and chloride loads for rainfall-initiated summer and fall events, and (2) the long-term hydrometric data was high-frequency and was analyzed/interpreted at the scale of individual rainfall-runoff events. The event-scale analyses performed on long-term data presented in this paper were facilitated by the quasi-automated rainfall-runoff event delineation tool HydRun. Tools that expedite tedious and subjective tasks (e.g., rainfall-runoff event delineation) present opportunities for analyses of long-term data that were previously impractical. These opportunities articulate secondary and tertiary benefits to collecting long-term, high-frequency hydrometric and chemistry data.

In this study, the high-frequency hydrometric data was essential for capturing temporal variability in hydrologic response, as these catchments have relatively small drainage areas (12-170 ha) and considerable upland bedrock exposure, which both contribute to flashy event responses. Combined, the data temporal resolution and the sensitivity of rainfall-runoff event detection associated with HydRun led to the consideration of a range of rainfall-runoff events, including smaller events that are often ignored in manual event delineation (Tarasova et al., 2018). The breadth of events captured in this study is articulated by the considerable temporal variability expressed by relatively large coefficients of variation for response magnitude metrics (Table 1). Additionally, the long-term data captured over multiple seasons is a strong contributor to the diversity of rainfall-runoff events observed in this study. This data captures a range of inter-annual conditions, which makes the presented analyses more resistant to specific annual or multi-year conditions (i.e., wet or dry) that are expressed in shorter-term data. Also, this data is less affected by extreme events that are likely to be characterized in field efforts conducted over shorter periods. These archetypal features of the hydrometric data that were used in this study led to the identification of limitations related to the lower-frequency chemistry data. The chemistry data were too sparse to estimate solute loads from paired chemistry and discharge data directly. Therefore, site- and season-specific regression models were developed to estimate daily solute loads that were summed over event durations to obtain event-specific load estimates. While these models were calibrated using grab sample data covering a wide range of hydrologic response conditions (Figure S1), this approach assumes that constituent concentrations of grab samples were representative of the average conditions of the day that they were collected. Indeed, similar

models have been used to predict solute concentrations or loads in a range of studies (e.g., Leigh et al., 2019; Long et al., 2015; Runkel et al., 2004) and here, the level of fit obtained during model calibration was relatively high. With that said, this approach does not allow for finer solute export dynamics, like first flush and hysteresis, to be characterized or associated with rapid fluctuations in hydrologic response (Inamdar et al., 2004, 2006; Inamdar & Mitchell, 2006).

Considerable inter-event variability in response magnitude was observed for the three catchments of this study (Table 1). This is consistent with most multi-year hydrometric data and is further corroborated by inter-event variability in response magnitude observed at another IISD-ELA catchment (Oswald et al., 2011; Ross et al., 2019). However, among the event-specific response magnitude metrics considered in this study, Q_{TOT}, Q_{MAX}, and I_{abs} were more variable than RR, indicating that the conversion efficiency of rainfall to runoff was less variable than other aspects of response magnitude. Overall, relatively low variability in event response timing was observed in this study (Table 2), except for timing metrics associated with the initiation of runoff (i.e., T_r and T_{LR}). Combined with higher variability in I_{abs}, these findings suggest that the volume and time needed to satisfy catchment storage before runoff initiation are critical aspects of hydrologic response at the study catchments (Dingman, 2015). Overall, similar event responses were observed among sites. Notably, for the NEIF, event T_r was shorter and less variable than other sites (Table 1), possibly a result of its comparatively small drainage area. In terms of seasonality, studies for other headwater boreal Shield catchments have suggested strong seasonal variability in hydrologic regime and runoff generation mechanisms resulting from differences in antecedent water table levels and storm duration and intensity (Frisbee et al., 2007). Similarly, differences in summer and fall event responses at another boreal Shield catchment were pronounced for some measures of response magnitude (e.g., RR) and were attributed to the influence of potential evapotranspiration during summer months on catchment storage (Allan & Roulet, 1994; Oswald et al., 2011). In the current study, statistically significant differences in catchment response between summer and fall events were only observed for select response metrics at the NEIF. While this is discongruous with the literature, this aspect of the analysis may have yielded different results if winter and spring events were considered in addition to summer and fall events.

Solute export at the catchment outlet can be conceptualized as the interaction between hydrological transport and biogeochemical processing across the catchment (Lohse et al., 2009). It can be difficult to untangle the relative importance of each set of drivers, given that they are both controlled by state factors including climate, geology, soil depth and type, and topography (Devito et al., 1999). Indeed, previous work on dissolved organic carbon and mercury at the IISD-ELA has attributed differences in solute export to antecedent moisture conditions, but without being able to resolve if the mechanism was due to differences in flowpaths or differences in catchment sources (Oswald et al., 2011). The significant differences observed among event response types suggests that considering timing metrics, such as T_r in addition to event magnitude can help illuminate sources of variability in solute export. High magnitude-slow timing events led to greater solute export compared with high magnitude-fast timing events, which may suggest that flowpaths and solute transport vary with event intensity (Indamdar et al., 2004). This was true for both NO_3-N and Cl, despite differences in the biological reactivity of the two ions. This may indicate that transport processes dominate over differences in source dynamics in these catchments, in contrast to cross-site comparisons which have found that NO_3-N dynamics of pristine catchments such as the ones in the present study tend to be controlled

more by biogeochemical processing compared with anthropogenically impacted sites (Basu et al., 2011). Differences across event response types were also consistent across catchments, despite physiographic differences among the three study sites, such as size and wetland coverage, and despite significant differences in the magnitude of solute export, suggesting that these patterns are somewhat robust to landscape variability in these boreal forested systems. Coupling long-term discharge records with higher frequency chemistry measurements will help to resolve the explanations for the patterns.

5 Conclusions

This work contributes to our understanding of relationships between hydrologic response and solute export in boreal Shield catchments. Rainfall-runoff event analysis of long-term hydrometric and chemistry data for three boreal Shield catchments indicated highly variable event hydrologic responses and NO_3-N and Cl loads. Temporal variability in hydrologic response was greatest for aspects of response related to the initiation of catchment runoff. This analysis also showed significant differences in event NO_3-N and Cl loads among sites, articulating the need for site-specific analyses. The focus on rainfall-runoff events spanning summer and fall months showed that seasonal differences in hydrologic response were only statistically significant for a small number of response metrics. In contrast, differences in NO_3-N and Cl loads for summer and fall events were statistically significant for most sites. This suggests there is considerable variability in response among seasons influenced by rainfall-initiated hydrologic events, demonstrating a need for more studies that evaluate rainfall-driven dynamics in regions that are expected to experience shifts in hydrologic regime due to stressors from climate change.

The use of an empirical classification space indicated that event responses for these boreal Shield catchments were dominantly low-magnitude and fast-timing. By synthesizing this event hydrologic response classification with estimates of event nitrate and chloride loads, this study showed statistically significant differences in solute loads between events of different response classes. It may be insightful for future studies to assess this classification framework for assessing solute export relative to dominant event hydrologic response in other contexts. Overall, analyses presented in this study leveraged newly available tools for quasi-automated rainfall-runoff event delineation that increase opportunities for evaluating long-term data at different timescales. Climate projections for this region include longer snow-free seasons, and increased frequency and intensity of storms and droughts (Collins et al. 2013) which will alter hydrological dynamics and solute transport across the heterogenous landscape of the boreal (Ducharme et al. 2021). These results demonstrate the need for long-term, high frequency hydrometric and chemical data collection in order to understand how shifting storm behaviour may alter solute transport in these sensitive ecosystems.

Acknowledgments

This work would not have been possible without the hard work and dedication of IISD-ELA staff and students, both past and present. In particular, we thanks Ken Sandilands and Paul Fafard for providing the high-frequency discharge data and for answering questions about data collection and processing. This work was funded by an NSERC Discovery Grant to NJC.

Discharge and stream chemistry data have been made publicly available by the IISD-ELA and are accessible through the DataStream data repository: https://doi.org/10.25976/r3kp-7m22. Rainfall data are publicly available by request to Environment and Climate Change Canada.

References

Allan, C. J., Roulet, N. T., & Hill, A. R. (1993). The Biogeochemistry of Pristine, Headwater Precambrian Shield Watersheds: An Analysis of Material Transport within a Heterogeneous Landscape. *Biogeochemistry*, *22*(1), 37–79.

Allan, Craig J., & Roulet, N. T. (1994). Runoff generation in zero-order precambrian shield catchments: The stormflow response of a heterogeneous landscape. *Hydrological Processes*, *8*(4), 369–388. https://doi.org/10.1002/hyp.3360080409

Basu, N. B., Destouni, G., Jawitz, J. W., Thompson, S. E., Loukinova, N. V., Darracq, A., Zanardo, S., Yaeger, M., Sivapalan, M., Rinaldo, A., & Rao, P. S. C. (2010). Nutrient loads exported from managed catchments reveal emergent biogeochemical stationarity. *Geophysical Research Letters*, *37*(23). https://doi.org/10.1029/2010GL045168

Basu, N. B., Thompson, S. E., & Rao, P. S. C. (2011). Hydrologic and biogeochemical functioning of intensively managed catchments: A synthesis of top-down analyses. *Water Resources Research*, *47*(10). https://doi.org/10.1029/2011WR010800

Blume, T., Zehe, E., & Bronstert, A. (2007). Rainfall—Runoff response, event-based runoff coefficients and hydrograph separation. *Hydrological Sciences Journal*, *52*(5), 843–862. https://doi.org/10.1623/hysj.52.5.843

Branfireun, B. A., & Roulet, N. T. (1998). The baseflow and storm flow hydrology of a precambrian shield headwater peatland. *Hydrological Processes*, *12*(1), 57–72. https://doi.org/10.1002/(SICI)1099-1085(199801)12:1<57::AID-HYP560>3.0.CO;2-U

Brunskill, G. J., & Schindler, D. W. (1971). Geography and Bathymetry of Selected Lake Basins, Experimental Lakes Area, Northwestern Ontario. *Journal of the Fisheries Research Board of Canada*, *28*(2), 139–155. https://doi.org/10.1139/f71-028

Carey, S. K., Tetzlaff, D., Seibert, J., Soulsby, C., Buttle, J., Laudon, H., McDonnell, J., McGuire, K., Caissie, D., Shanley, J., Kennedy, M., Devito, K., & Pomeroy, J. W. (2010). Inter-comparison of hydro-climatic regimes across northern catchments: Synchronicity, resistance and resilience. *Hydrological Processes*, *24*(24), 3591–3602. https://doi.org/10.1002/hyp.7880

Carey, S. K., & Woo, M. (2001). Slope runoff processes and flow generation in a subarctic, subalpine catchment. *Journal of Hydrology*, *253*(1–4), 110–129.

Casson, N. J., Eimers, M. C., & Watmough, S. A. (2012). Impact of winter warming on the timing of nutrient export from forested catchments. *Hydrological Processes*, *26*(17), 2546–2554. https://doi.org/10.1002/hyp.8461

Casson, Nora J., Eimers, M. C., Watmough, S. A., & Richardson, M. C. (2019). The role of wetland coverage within the near-stream zone in predicting of seasonal stream export chemistry from forested headwater catchments. *Hydrological Processes*, *33*(10), 1465–1475. https://doi.org/10.1002/hyp.13413

Cirmo, C. P., & McDonnell, J. J. (1997). Linking the hydrologic and biogeochemical controls of nitrogen transport in near-stream zones of temperate-forested catchments: A review. *Journal of Hydrology*, *199*(1), 88–120. https://doi.org/10.1016/S0022-1694(96)03286-6

Collins, M., Knutti, R., Arblaster, J., Dufresne, J.-L., Fichefet, T., Friedlingstein, P., … Booth, B. B. B. (2013). Long-term Climate Change: Projections, Commitments and Irreversibility. *Climate Change 2013 - The Physical Science Basis: Contribution of Working Group I to*

the Fifth Assessment Report of the Intergovernmental Panel on Climate Change, 1029–1136.

Creed, I. F., & Band, L. E. (1998). Export of nitrogen from catchments within a temperate forest: Evidence for a unifying mechanism regulated by variable source area dynamics. *Water Resources Research*, *34*(11), 3105–3120. https://doi.org/10.1029/98WR01924

Creed, I. F., Band, L. E., Foster, N. W., Morrison, I. K., Nicolson, J. A., Semkin, R. S., & Jeffries, D. S. (1996). Regulation of Nitrate-N Release from Temperate Forests: A Test of the N Flushing Hypothesis. *Water Resources Research*, *32*(11), 3337–3354. https://doi.org/10.1029/96WR02399

Devito, K., Creed, I., Gan, T., Mendoza, C., Petrone, R., Silins, U., & Smerdon, B. (2005). A framework for broad-scale classification of hydrologic response units on the Boreal Plain: Is topography the last thing to consider? *Hydrological Processes, 19*(8), 1705–1714. https://doi.org/10.1002/hyp.5881

Devito, K. J., Westbrook, C. J., & Schiff, S. L. (1999). Nitrogen mineralization and nitrification in upland and peatland forest soils in two Canadian Shield catchments. *Canadian Journal of Forest Research*, *29*(11), 1793–1804.

Dingman, S. L. (2015). *Physical hydrology*. Waveland press.

Ducharme, A. A., Casson, N. J., Higgins, S. N., & Friesen-Hughes, K. (2021) Hydrological and catchment controls on event-scale dissolved organic carbon dynamics in boreal headwater streams. *Hydrological Processes, 35*(7), e14279.

Duncan, J. M., Band, L. E., & Groffman, P. M. (2017). Variable nitrate concentration–discharge relationships in a forested watershed. *Hydrological Processes*, *31*(9), 1817–1824. https://doi.org/10.1002/hyp.11136

Eimers, M. C., Buttle, J., & Watmough, S. A. (2011). Influence of seasonal changes in runoff and extreme events on dissolved organic carbon trends in wetland- and upland-draining streams. *Canadian Journal of Fisheries and Aquatic Sciences*. https://doi.org/10.1139/f07-194

Emmerton, C. A., Beaty, K. G., Casson, N. J., Graydon, J. A., Hesslein, R. H., Higgins, S. N., Osman, H., Paterson, M. J., Park, A., & Tardif, J. C. (2019). Long-term responses of nutrient budgets to concurrent climate-related stressors in a Boreal Watershed. *Ecosystems*, *22*(2), 363–378.

Frisbee, M. D., Allan, C. J., Thomasson, M. J., & Mackereth, R. (2007). Hillslope hydrology and wetland response of two small zero-order boreal catchments on the Precambrian Shield. *Hydrological Processes*, *21*(22), 2979–2997. https://doi.org/10.1002/hyp.6521

Godsey, S. E., Kirchner, J. W., & Clow, D. W. (2009). Concentration–discharge relationships reflect chemostatic characteristics of US catchments. *Hydrological Processes: An International Journal*, *23*(13), 1844–1864.

Hollander, M., Wolfe, D. A., & Chicken, E. (2013). *Nonparametric statistical methods* (Vol. 751). John Wiley & Sons.

Horowitz, A. J. (2013). A Review of Selected Inorganic Surface Water Quality-Monitoring Practices: Are We Really Measuring What We Think, and If So, Are We Doing It Right? *Environmental Science & Technology*, *47*(6), 2471–2486. https://doi.org/10.1021/es304058q

Inamdar, S., Christopher, S. F., & Mitchell, M. J. (2004). Export mechanisms for dissolved organic carbon and nitrate during summer storm events in a glaciated forested catchment

in New York, USA. *Hydrological Processes*, *18*(14), 2651–2661. https://doi.org/10.1002/hyp.5572

Inamdar, S., & Mitchell, M. J. (2006). Hydrologic and topographic controls on storm-event exports of dissolved organic carbon (DOC) and nitrate across catchment scales. *Water Resources Research*, *42*(3). https://doi.org/10.1029/2005WR004212

Inamdar, S., O'leary, N., Mitchell, M. J., & Riley, J. T. (2006). The impact of storm events on solute exports from a glaciated forested watershed in western New York, USA. *Hydrological Processes: An International Journal*, *20*(16), 3423–3439.

Jager, D. F., Wilmking, M., & Kukkonen, J. V. K. (2009). The influence of summer seasonal extremes on dissolved organic carbon export from a boreal peatland catchment: Evidence from one dry and one wet growing season. *Science of The Total Environment*, *407*(4), 1373–1382. https://doi.org/10.1016/j.scitotenv.2008.10.005

James, A., & Roulet, N. (2007). Investigating hydrologic connectivity and its association with threshold change in runoff response in a temperate forested watershed. *Hydrological Processes*, *21*(25), 3391–3408. https://doi.org/10.1002/hyp.6554

Legendre, P., & Legendre, L. F. (2012). *Numerical ecology* (Vol. 24). Elsevier. https://books.google.ca/books?hl=en&lr=&id=6ZBOA-iDviQC&oi=fnd&pg=PP1&dq=numerical+ecology&ots=uy5n-7Q2Rj&sig=bb5FDdZPoNsGVpgcJTt8lvKZKqs

Leigh, C., Kandanaarachchi, S., McGree, J. M., Hyndman, R. J., Alsibai, O., Mengersen, K., & Peterson, E. E. (2019). Predicting sediment and nutrient concentrations from high-frequency water-quality data. *PloS One*, *14*(8), e0215503.

Lohse, K. A., Brooks, P. D., McIntosh, J. C., Meixner, T., & Huxman, T. E. (2009). Interactions between biogeochemistry and hydrologic systems. *Annual Review of Environment and Resources*, *34*, 65–96.

Long, T., Wellen, C., Arhonditsis, G., Boyd, D., Mohamed, M., & O'Connor, K. (2015). Estimation of tributary total phosphorus loads to Hamilton Harbour, Ontario, Canada, using a series of regression equations. *Journal of Great Lakes Research*, *41*(3), 780–793.

Macrae, M. L., English, M. C., Schiff, S. L., & Stone, M. (2007). Capturing temporal variability for estimates of annual hydrochemical export from a first-order agricultural catchment in southern Ontario, Canada. *Hydrological Processes*, *21*(13), 1651–1663. https://doi.org/10.1002/hyp.6361

McClain, M. E., Boyer, E. W., Dent, C. L., Gergel, S. E., Grimm, N. B., Groffman, P. M., Hart, S. C., Harvey, J. W., Johnston, C. A., Mayorga, E., McDowell, W. H., & Pinay, G. (2003). Biogeochemical Hot Spots and Hot Moments at the Interface of Terrestrial and Aquatic Ecosystems. *Ecosystems*, *6*(4), 301–312. https://doi.org/10.1007/s10021-003-0161-9

McDonnell, J., Sivapalan, M., Vaché, K., Dunn, S., Grant, G., Haggerty, R., Hinz, C., Hooper, R., Kirchner, J., Roderick, M. L., Selker, J., & Weiler, M. (2007). Moving beyond heterogeneity and process complexity: A new vision for watershed hydrology. *Water Resources Research*, *43*(7), W07301. https://doi.org/10.1029/2006WR005467

McGlynn, B. L., & McDonnell, J. (2003). Quantifying the relative contributions of riparian and hillslope zones to catchment runoff. *Water Resources Research*, *39*(11), 1310. https://doi.org/10.1029/2003WR002091

Moatar, F., Abbott, B. W., Minaudo, C., Curie, F., & Pinay, G. (2017). Elemental properties, hydrology, and biology interact to shape concentration-discharge curves for carbon, nutrients, sediment, and major ions. *Water Resources Research*, *53*(2), 1270–1287. https://doi.org/10.1002/2016WR019635

Oswald, C. J., & Branfireun, B. A. (2014). Antecedent moisture conditions control mercury and dissolved organic carbon concentration dynamics in a boreal headwater catchment. *Water Resources Research*, *50*(8), 6610–6627. https://doi.org/10.1002/2013WR014736

Oswald, C., Richardson, M. C., & Branfireun, B. A. (2011). Water storage dynamics and runoff response of a boreal Shield headwater catchment. *Hydrological Processes*, *25*(19), 3042–3060. https://doi.org/10.1002/hyp.8036

Parker, B. R., Schindler, D. W., Beaty, K. G., Stainton, M. P., & Kasian, S. E. (2009). Long-term changes in climate, streamflow, and nutrient budgets for first-order catchments at the Experimental Lakes Area (Ontario, Canada). *Canadian Journal of Fisheries and Aquatic Sciences*, *66*(11), 1848–1863.

Pellerin, B. A., Saraceno, J. F., Shanley, J. B., Sebestyen, S. D., Aiken, G. R., Wollheim, W. M., & Bergamaschi, B. A. (2012). Taking the pulse of snowmelt: In situ sensors reveal seasonal, event and diurnal patterns of nitrate and dissolved organic matter variability in an upland forest stream. *Biogeochemistry*, *108*(1–3), 183–198.

Raymond, P. A., & Saiers, J. E. (2010). Event controlled DOC export from forested watersheds. *Biogeochemistry*, *100*(1), 197–209. https://doi.org/10.1007/s10533-010-9416-7

Ross, C. A., Ali, G., Spence, C., Oswald, C., & Casson, N. (2019). Comparison of event-specific rainfall–runoff responses and their controls in contrasting geographic areas. *Hydrological Processes*, *33*(14), 1961–1979. https://doi.org/10.1002/hyp.13460

Runkel, R. L., Crawford, C. G., & Cohn, T. A. (2004). *Load Estimator (LOADEST): A FORTRAN program for estimating constituent loads in streams and rivers*.

Schindler, D. W., Bayley, S. E., Parker, B. R., Beaty, K. G., Cruikshank, D. R., Fee, E. J., Schindler, E. U., & Stainton, M. P. (1996). The effects of climatic warming on the properties of boreal lakes and streams at the Experimental Lakes Area, northwestern Ontario. *Limnology and Oceanography*, *41*(5), 1004–1017.

Stieglitz, M., Shaman, J., McNamara, J., Engel, V., Shanley, J., & Kling, G. W. (2003). An approach to understanding hydrologic connectivity on the hillslope and the implications for nutrient transport. *Global Biogeochemical Cycles*, *17*(4). https://doi.org/10.1029/2003GB002041

Swistock, B. R., Edwards, P. J., Wood, F., & Dewalle, D. R. (1997). Comparison of methods for calculating annual solute exports from six forested Appalachian watersheds. *Hydrological Processes*, *11*(7), 655–669.

Tang, W., & Carey, S. K. (2017). HydRun: A MATLAB toolbox for rainfall–runoff analysis. *Hydrological Processes*, *31*(15), 2670–2682. https://doi.org/10.1002/hyp.11185

Tarasova, L., Basso, S., Zink, M., & Merz, R. (2018). Exploring Controls on Rainfall-Runoff Events: 1. Time Series-Based Event Separation and Temporal Dynamics of Event Runoff Response in Germany. *Water Resources Research*, *54*(10), 7711–7732. https://doi.org/10.1029/2018WR022587

Te Chow, V. (1959). *Open-channel hydraulics* (Vol. 1). McGraw-Hill New York.

Vargha, A., & Delaney, H. D. (1998). The Kruskal-Wallis test and stochastic homogeneity. *Journal of Educational and Behavioral Statistics*, *23*(2), 170–192.

Whitfield, P. H., & Cannon, A. J. (2000). Recent Variations in Climate and Hydrology in Canada. *Canadian Water Resources Journal / Revue Canadienne Des Ressources Hydriques*, *25*(1), 19–65. https://doi.org/10.4296/cwrj2501019

Woo, M., Thorne, R., Szeto, K., & Yang, D. (2008). Streamflow hydrology in the boreal region under the influences of climate and human interference. *Philosophical Transactions of the Royal Society B: Biological Sciences*, *363*(1501), 2249–2258. https://doi.org/10.1098/rstb.2007.2197